

Cambridge University Press & Assessment

978-1-605-11652-5 — Synthesis, Characterization, and Applications of Functional Materials

Edited by Valentin Craciun , Maryline Guilloux-Viry , Menka Jain , Quanxi Jia , Hiromitsu Kozuka ,  
Dhananjay Kumar , Sanjay Mathur , Xavier Obradors , Kaushal K. Singh

Excerpt

[More Information](#)

---

## **ZnO Thin Films and Nanostructures**

Mater. Res. Soc. Symp. Proc. Vol. 1675 © 2014 Materials Research Society

DOI: 10.1557/opl.2014.860

### Optimization of Annealing Conditions for ZnO-based Thin Films Grown Using MOCVD

Anas Mazady, Abdiel Rivera, and Mehdi Anwar

*Electrical and Computer Engineering, University of Connecticut, Storrs, CT 06269, Email: anwara@engr.uconn.edu*

#### ABSTRACT

In this work, effects of thermal annealing on the structural and optical properties of ZnO thin films grown on p-Si and GaN substrates using metalorganic chemical vapor deposition (MOCVD) are investigated. Annealing at 600 °C results in optimum crystal and optical qualities of the ZnO thin films on both substrates. Smaller lattice mismatch between grown ZnO epitaxial layer on GaN substrates results in better film morphology as compared to p-Si substrates. Higher annealing temperature along with a slower thermal ramp provides better crystal quality of ZnO thin films on both substrates. Annealing ZnO thin films at 700 °C with a slower thermal ramp results in better crystal quality as is evident from a 56% reduction in the full-width at half maximum (FWHM) of the (002) peak compared to the as-grown films. The optical quality also enhances with a slower annealing rate. The determination of the optimum annealing conditions for different substrates has important implications in fabricating optimized and efficient ZnO based electronics.

#### INTRODUCTION

ZnO, being a transparent conductive oxide, has drawn considerable interests in fabricating transparent electrodes for display devices, transparent electronics, and photovoltaic devices, to name a few [1]. A large direct bandgap energy of 3.37 eV makes it an ideal candidate for optoelectronic applications, such as, solar blind ultra-violet (UV) detectors, UV diodes, LEDs, among others. Reasonable smaller lattice mismatch of 2% with GaN also allows ZnO to be a good substrate material for GaN based devices, as stand-alone GaN substrates are not available yet [2]. Being resistant to radiation damage, compared with other semiconductors, makes ZnO a suitable candidate for space applications [3].

The large lattice mismatch of 40% and large difference in the thermal expansion coefficients of 87% between ZnO and Si substrates cause built-in residual stress in the grown ZnO NWs. Proper annealing conditions can reduce this built-in residual stress and hence can improve the crystalline quality and minimize defects of the grown ZnO NWs. Post annealing not only passivates native defects but also improves the near band-edge emission of ZnO films through reduction of non-radiative recombination centers in the films [4]. It also produced a smooth surface of the film required for most optoelectronic application. Sengupta et al. [5] investigated the annealing effects on ZnO film grown via sol-gel. They observed that the intensity of (002) peak gradually increases with increasing annealing temperature, giving rise to a smaller full width at half maxima (FWHM) and an average larger grain size. This phenomenon is attributed to the thermal annealing induced coalescence of small grains by grain boundary diffusion, resulting in larger grain size [6].

In this work, effects of thermal annealing on the structural and optical properties of ZnO thin films grown using metalorganic chemical vapor deposition (MOCVD) are investigated. Mahmood et al. [7] performed similar studies on ZnO thin films deposited using reactive e-beam evaporation technique. However, material quality can be significantly improved by employing MOCVD which is also a standard technique for mass production in the industries.

## EXPERIMENT

ZnO thin films were deposited on p-Si and GaN substrates using FirstNano EasyTube 3000 MOCVD system at a constant temperature and pressure of 300 °C and 70 Torr, respectively. Diethylzinc (DEZn) and N<sub>2</sub>O were used as the zinc and oxygen precursors and nitrogen was used as the carrier gas. The growth was carried out for 20 mins maintaining a steady flow of 50 SCCM and 35 SCCM of DEZn and N<sub>2</sub>O, respectively. After deposition of the thin film, the samples were annealed at 500 – 750 °C under N<sub>2</sub> ambient.

## DISCUSSION

The scanning electron microscope (SEM) images of ZnO thin films grown on p-Si substrates are shown in Figure 1. The as-grown film on p-Si substrate shows granular surface texture with very fine grains. Thermal annealing treatments at 500 and 600 °C result in a smoother film with smaller RMS roughness. For annealing temperatures higher than 700 °C, large grains were visible with the grain size varying between 35 and 155 nm. In contrast, ZnO thin films grown on GaN substrates showed better morphology in general, as shown in Figure 2, which is attributed to a smaller lattice mismatch between ZnO and GaN. For comparison, the lattice mismatch exerts a 40% tensile strain on ZnO thin films grown on p-Si substrates, whereas the strain is only 2% (compressive) in the case of ZnO thin films grown on GaN substrates. Annealing at temperatures higher than 600 °C resulted in a very smooth surface of the film on GaN substrates.

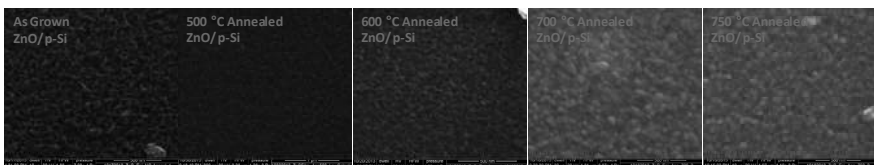


Figure 1. SEM images of ZnO (thin film) on p-Si substrates

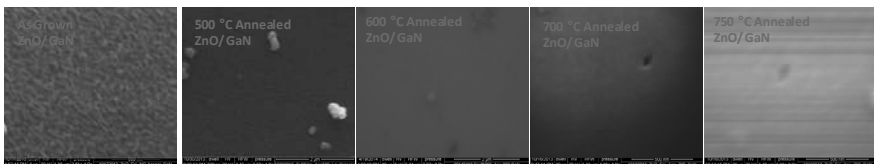


Figure 2. SEM images of ZnO (thin film) on GaN substrates

In order to investigate the origin of the granular textures, the samples were annealed and cooled at a slower rate of 2.5 °C/min which is twice as slower than the regular annealing condition used in this study. SEM images of the thin film annealed at different rates and temperatures are shown in Figure 3. The slower annealing/ cooling rate did not show any observable difference in the grain size of ZnO thin films on different substrates compared to their faster annealed counterparts. This suggests that the observed granular surface texture at higher annealing temperature is not a direct result of the thermal coefficient mismatch. Rather, at high annealing temperatures the grain boundaries migrate and the adjacent grains coalesce, independent of the annealing/ cooling ramp [8].

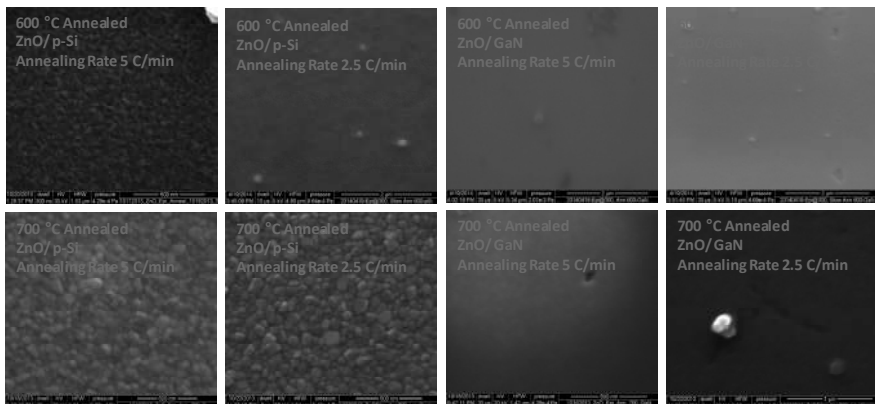


Figure 3. Slow Vs. fast annealing/cooling ramp for ZnO thin film grown on p-Si and GaN substrates

Figure 4 shows X-ray diffraction (XRD) measurement results of ZnO thin films of p-Si substrates. The as-grown film has multiple growth facets, along (100), (002), and (200). The film became more single crystalline with (002) orientation, when annealed at 600 °C. It is also important to note that, although a slow annealing does not affect the morphology, it improves the crystalline quality significantly. It is clear from the figure that the (002) peak has a much higher intensity than the other peaks for the samples annealed/ cooled at a slower thermal ramp than those at a faster ramp.

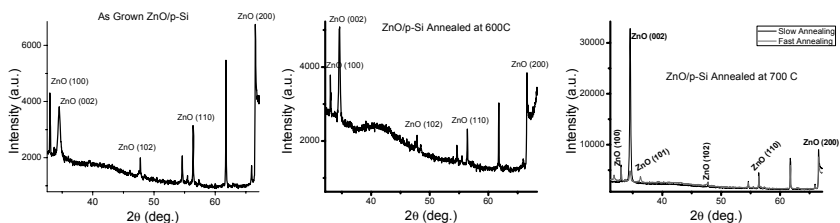


Figure 4. XRD measurement results of ZnO thin film grown on p-Si substrates

Table 1. Summary of crystalline quality of ZnO thin film on p-Si substrates annealed at different temperatures

	As-Grown	500 °C	600 °C	700 °C Slow	700 °C Fast
<b>c-lattice (Å)</b>	5.1921	5.1906	5.1820	5.1870	5.1891
<b>a-lattice (Å)</b>	3.2430	3.2430	3.2406	3.1792	3.2417
<b>Misfit Strain</b>	67.47%	67.47%	67.59%	70.83%	67.53%
<b>FWHM (deg)</b>	0.2225	0.1279	0.1280	0.09695	0.1239

Table 1 summarizes the crystalline quality of ZnO thin films grown on p-Si substrates and annealed at different temperatures. The c-lattice constant is observed to decrease with increased annealing temperature which is in agreement with the observations made by other groups [9–11]. Comparison of the full width at half maximum (FWHM) of the (002) peak suggests that the crystalline quality becomes better with higher temperature annealing and a slower anneal/ cooling ramp increases the film quality to a higher degree. For an example, the 700 °C slow annealed sample has a 56% smaller FWHM than the as-grown film.

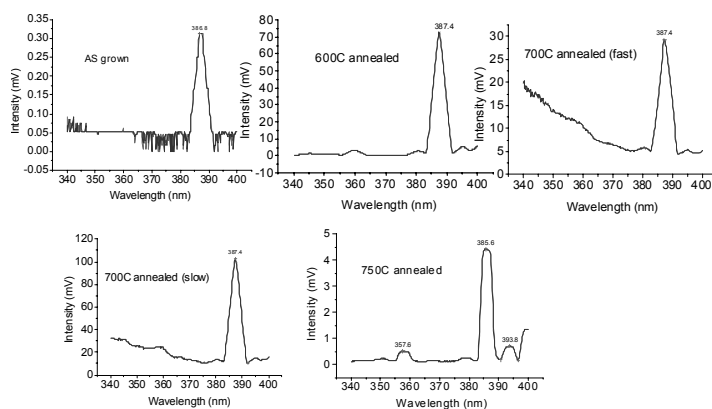


Figure 5. Room temperature photoluminescence (PL) spectra of ZnO/p-Si thin films annealed at different temperatures

Room temperature photoluminescence (PL) spectra of ZnO thin films annealed at different temperatures are shown in Figure 5. A He-Cd laser line at 325 nm was used to excite the samples, and a monochromator, optical chopper, and lock-in amplifier assembly was employed in standard configuration for the detection of the PL spectra. The most dominant peak was observed at ~387.4 nm corresponding to near band-edge (NBE) emission of free excitons. The FWHM of the NBE peak was measured to be 5.21, 4.38, 5.21, 4.79, and 4.38 nm, respectively, for the as-grown, 600 °C, 700 °C (fast), 700 °C (slow), and 750 °C annealed samples. Annealing at 600 °C obtained the smallest FWHM of 4.38 nm among all the p-Si samples which is also 16% smaller than the as-grown p-Si samples. The 750 °C annealed sample also had a 4.38°

FWHM of the NBE peak, but another peak at 358 nm emerges, which is due to the band to band transition of electrons [12].

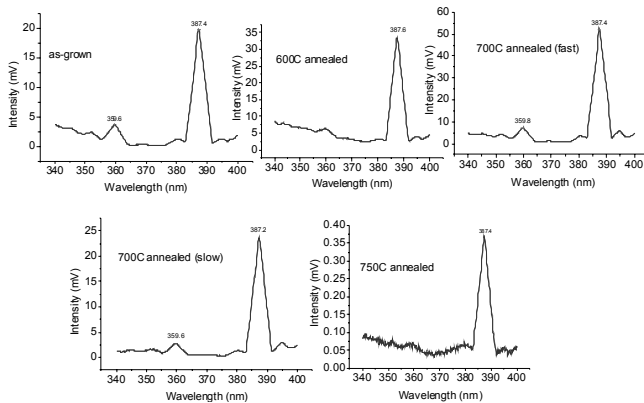


Figure 6. Room temperature photoluminescence (PL) spectra of ZnO/GaN thin films annealed at different temperatures

PL spectra of ZnO thin films grown on GaN substrates and annealed at different temperatures are shown in **Error! Reference source not found.** FWHM of ZnO/GaN thin films are determined to be 4.58, 4.58, 4.79, 4.58, and 4.79 nm, respectively. The peak intensity of the 600 °C annealed ZnO/GaN sample was 69% higher than the as-grown film. All the measurements therefore suggest 600 °C to be the optimum annealing temperature for ZnO thin films grown on both p-Si and GaN substrates.

## CONCLUSIONS

ZnO thin films were grown on p-Si and GaN substrates using MOCVD. The films were annealed at 500, 600, 700, and 750 °C at different anneal/ cooling rates under N<sub>2</sub> ambient, *in situ* in the process chamber. Least surface roughness of the ZnO/p-Si thin films was obtained when annealed at 500-600 °C window. GaN substrates obtain better morphology of ZnO thin films than p-Si substrates due to a smaller lattice mismatch. Higher annealing temperature with a slower thermal ramp obtains better crystal quality of ZnO thin films on both substrates. Optical quality also enhances for a slower annealing rate.

## ACKNOWLEDGMENTS

The research was partially supported by NSF I/UCRC, Magnolia Optical Technologies, Inc., NAVAIR, Department of Education, and the Center for Hardware Assurance, Security, and Engineering (CHASE). The authors would like to acknowledge the support of Drs. Ashok Sood, Tariq Manzur and John Zeller.

## REFERENCES

- [1] X. Jiang, F. Wong, M. Fung and S. Lee, "Aluminum-doped zinc oxide films as transparent conductive electrode for organic light-emitting devices," *Appl. Phys. Lett.*, vol. 83, pp. 1875-1877, 2003.
- [2] Z. Chen, S. Yamamoto, M. Maekawa, A. Kawasuso, X. Yuan and T. Sekiguchi, "Postgrowth annealing of defects in ZnO studied by positron annihilation, x-ray diffraction, Rutherford backscattering, cathodoluminescence, and Hall measurements," *J. Appl. Phys.*, vol. 94, pp. 4807-4812, 2003.
- [3] D. C. Look, D. Reynolds, J. W. Hemsky, R. Jones and J. Sizelove, "Production and annealing of electron irradiation damage in ZnO," *Appl. Phys. Lett.*, vol. 75, pp. 811-813, 1999.
- [4] Y. Wang, S. Lau, X. Zhang, H. Hng, H. Lee, S. Yu and B. Tay, "Enhancement of near-band-edge photoluminescence from ZnO films by face-to-face annealing," *J. Cryst. Growth*, vol. 259, pp. 335-342, 2003.
- [5] J. Sengupta, R. Sahoo, K. Bardhan and C. Mukherjee, "Influence of annealing temperature on the structural, topographical and optical properties of sol-gel derived ZnO thin films," *Mater Lett*, vol. 65, pp. 2572-2574, 2011.
- [6] Y. Caglar, S. Ilican, M. Caglar, F. Yakuphanoglu, J. Wu, K. Gao, P. Lu and D. Xue, "Influence of heat treatment on the nanocrystalline structure of ZnO film deposited on p-Si," *J. Alloys Compounds*, vol. 481, pp. 885-889, 2009.
- [7] A. Mahmood, N. Ahmed, Q. Raza, T. M. Khan, M. Mehmood, M. Hassan and N. Mahmood, "Effect of thermal annealing on the structural and optical properties of ZnO thin films deposited by the reactive e-beam evaporation technique," *Phys. Scripta*, vol. 82, pp. 065801, 2010.
- [8] Y. Lin, J. Xie, H. Wang, Y. Li, C. Chavez, S. Lee, S. Foltyn, S. Crooker, A. Burrell and T. McCleskey, "Green luminescent zinc oxide films prepared by polymer-assisted deposition with rapid thermal process," *Thin Solid Films*, vol. 492, pp. 101-104, 2005.
- [9] V. Gupta and A. Mansingh, "Influence of postdeposition annealing on the structural and optical properties of sputtered zinc oxide film," *J. Appl. Phys.*, vol. 80, pp. 1063-1073, 1996.
- [10] M. Puchert, P. Timbrell and R. Lamb, "Postdeposition annealing of radio frequency magnetron sputtered ZnO films," *Journal of Vacuum Science & Technology A*, vol. 14, pp. 2220-2230, 1996.
- [11] Y. Lee, S. Hu, W. Water, K. Tiong, Z. Feng, Y. Chen, J. Huang, J. Lee, C. Huang and J. Shen, "Rapid thermal annealing effects on the structural and optical properties of ZnO films deposited on Si substrates," *J Lumin*, vol. 129, pp. 148-152, 2009.
- [12] G. Lee, Y. Yamamoto, M. Kouroggi and M. Ohtsu, "Blue shift in room temperature photoluminescence from photo-chemical vapor deposited ZnO films," *Thin Solid Films*, vol. 386, pp. 117-120, 2001.

Mater. Res. Soc. Symp. Proc. Vol. 1675 © 2014 Materials Research Society

DOI: 10.1557/opl.2014.886

### ZnO Nanostructures on Electrospun Nanofibers by Atomic Layer Deposition/Hydrothermal Growth and Their Photocatalytic Activity

Fatma Kayaci,<sup>1,2</sup> Sessa Vempati,<sup>\*1</sup> Cagla Ozgit-Akgun,<sup>1,2</sup> Necmi Biyikli<sup>1,2</sup> and Tamer Uyar<sup>\*\*1,2</sup>

<sup>1</sup> UNAM-National Nanotechnology Research Center, Bilkent University, Ankara, 06800, Turkey

<sup>2</sup> Institute of Materials Science & Nanotechnology, Bilkent University, Ankara, 06800, Turkey

Authors for correspondence: \*svempati01@qub.ac.uk; \*\*uyar@unam.bilkent.edu.tr

#### ABSTRACT

A hierarchy of nanostructured-ZnO was fabricated on the electrospun nanofibers by atomic layer deposition (ALD) and hydrothermal growth, subsequently. Firstly, we produced poly(acrylonitrile) (PAN) nanofibers via electrospinning, then ALD process provided a highly uniform and conformal coating of polycrystalline ZnO with a precise control on the thickness (50 nm). In the last step, this ZnO coating depicting dominant oxygen vacancies and significant grain boundaries was used as a seed on which single crystalline ZnO nanoneedles (average diameter and length of ~25 nm and ~600 nm, respectively) with high optical quality were hydrothermally grown. The detailed morphological and structural studies were performed on the resulting nanofibers, and the photocatalytic activity (PCA) was tested with reference to the degradation of methylene blue. The results of PCA were discussed in conjunction with photoluminescence response. The nanoneedle structures supported the vectorial transport of photo-charge carriers, which is crucial for high catalytic activity. The enhanced PCA, structural stability and reusability of the PAN/ZnO nanoneedles indicated that this hierarchical structure is a potential candidate for waste water treatment.

#### INTRODUCTION

Development of novel materials with enhanced photocatalytic activity (PCA) along with stability is one of the intensely researched topics for water purification and waste treatment. The need for such research arises due to water pollution and ever increasing environmental issues threatening the human health severely [1-3]. Metal oxides such as ZnO in the structures of nanoparticles [4], nanorods [5, 6] and nanofibers [4] are widely studied for water purification purposes due to their well known PCA. On the other hand, electrospun polyacrylonitrile (PAN) nanofibers have been widely adopted in water filtration due to their unique properties including high surface area, nanoporous structure, low basis weight, easy permeability, good stability and chemical resistance [7-10]. Here we fabricated a hierarchy of nanostructured-ZnO depicting a synergy effect to enhance the PCA on electrospun PAN nanofibers using chemical vapor deposition and liquid phase deposition techniques, namely atomic layer deposition (ALD) and hydrothermal growth [11].

#### EXPERIMENTAL DETAILS

N,N-dimethylformamide (Pestanal, Riedel) was used as a solvent to prepare 12% (w/v) PAN (Mw: 150,000, Scientific Polymer Products, Inc.) solution. For the electrospinning of the PAN solution; feed rate, applied voltage and tip-to-collector distance were 1 mL/h, 15 kV and 12 cm, respectively. ZnO seed deposition on electrospun PAN nanofibers was carried out at ~200



°C in a Savannah S100 ALD reactor (Cambridge Nanotech Inc.) using diethylzinc (Sigma-Aldrich) and HPLC grade water as the zinc precursor and oxidant, respectively. N<sub>2</sub> was used as a carrier gas at a flow rate of ~20 sccm. 400 cycles were applied via exposure mode (a trademark of Ultratech/Cambridge Nanotech Inc.) in which dynamic vacuum was switched to static vacuum before each precursor pulse. For the growth of ZnO nanoneedles on 3.6 mg of PAN/ZnO seed by hydrothermal process (90 °C, 5 h) in crucible, equimolar (0.02 M) zinc acetate dihydrate (≥ 98%, Sigma-Aldrich) and hexamethylene tetramine (≥ 99%, Alfa Aesar) were used. The morphology of the samples was studied using a scanning electron microscope (SEM, FEI – Quanta 200 FEG) with a nominal 5 nm of Au/Pd sputter coating. Transmission electron microscope (TEM, FEI–Tecnai G2F30) images and selected area electron diffraction (SAED) pattern were also obtained. Photoluminescence (PL) measurements were performed using Horiba Scientific FL-1057 TCSPC at an excitation wavelength of 360 nm. Methylene blue (MB, Sigma-Aldrich, certified by the Biological Stain Commission) was used as a model organic dye to test PCA of the samples. The nanofibrous mats (weight: 3.6 mg) were immersed in quartz cuvettes containing the MB solution (18.8 μM). The cuvettes were exposed to UV light (300 W, Osram, Ultra-Vitalux, sunlight simulation) placed at a distance of ~15 cm. Dye concentrations in the cuvettes were measured using a UV-Vis-NIR spectrophotometer (Varian Cary 5000) at regular time intervals. We have repeated the PCA experiment twice (i.e. 2<sup>nd</sup> and 3<sup>rd</sup> cycles) for PAN/ZnO needle sample (~3.3 mg) to determine the reusability versus performance. All the figures are reproduced with permission from Ref [11]

## DISCUSSION

ZnO seed-coated PAN nanofibers were fabricated through electrospinning and ALD processes, on which ZnO nanoneedles were hydrothermally grown [11]. Schematic representations of the electrospinning and ALD processes, and fabrication procedure for the hierarchical PAN/ZnO needle nanofiber are illustrated in figure 1.

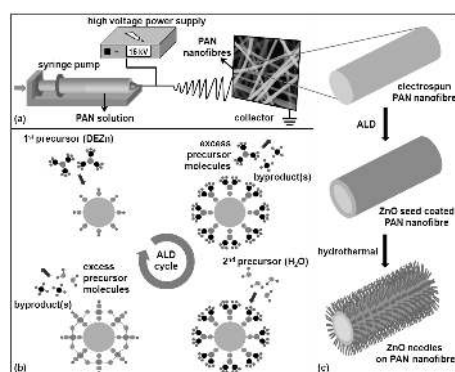


**Figure 1.** Schematic representations of the (a) electrospinning of PAN solution, (b) ALD of ZnO seed onto PAN nanofiber, and (c) fabrication procedure for hierarchical PAN/ZnO needle nanofiber.

The representative SEM images of PAN nanofibers are given in figure 2(a), where the average fiber diameter (AFD) is estimated to be  $\sim 655 \pm 135$  nm. After the ALD process, we have recorded the SEM images which are shown in figure 2(b) where the AFD is  $\sim 715 \pm 125$  nm. AFD increased because of ALD coating, and moreover the fiber structure was stable during the ALD process. Subsequently, the hydrothermal method was employed to grow ZnO nanoneedles on the ZnO seed-coated PAN nanofibers. Straight ZnO nanoneedles covered the surface of the ZnO seed-coated PAN nanofibers, and no branching was observed, figure 2(c1-2). By analyzing the figure 2(c2), average diameter and length of the nanoneedles were determined as  $\sim 25$  nm and  $\sim 600$  nm, respectively.

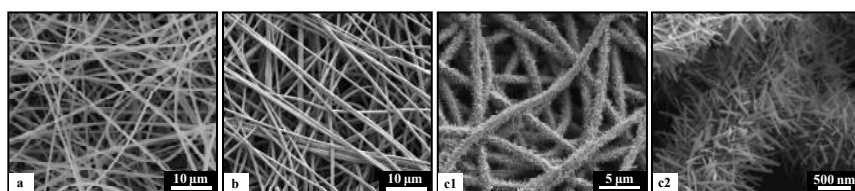


**Figure 2.** Representative SEM images of (a) pristine PAN, (b) PAN/ZnO seed, and (c1-2) PAN/ZnO needle nanofibers at different magnifications.

Despite the relatively large surface area of the nanofibers, the conformal coating of ZnO with a uniform thickness ( $\sim 50$  nm) was observed from the TEM image of PAN/ZnO seed nanofiber shown in figure 3(a1). For the high surface area substrates such as non-woven nanofiber mat, ALD is a well suitable technique as shown by us earlier [12, 13]. The SAED pattern in figure 3(a2) reveals the polycrystalline nature of ZnO seed. The bright spots on the polycrystalline diffraction rings were observed due to the presence of well crystalline grains [13]. Moreover, high resolution TEM (HRTEM) and fast Fourier transform (FFT) images indicate the single crystalline nature of ZnO nanoneedles (figure 3(b1), (b2)). It is important to determine the growth direction of ZnO; hence, the lattice spacing was measured as  $\sim 0.525$  nm corresponding to *c*-axis that is the preferential growth direction of the nanoneedles. Therefore polar planes of ZnO have shown to depict relatively higher PCA [14].

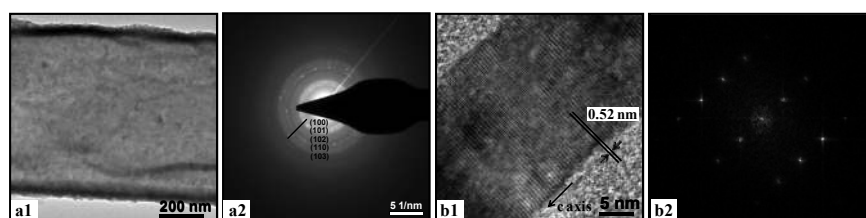


**Figure 3.** Representative (a1) TEM image and (a2) SAED pattern of PAN/ZnO seed nanofiber; (b1) HRTEM image and (b2) FFT image of ZnO needle.

We inferred the information about surface defects from the PL spectra of nanofibers (figure 4a); such defects play a crucial role in determining the PCA of the material. Based on the literature, various crystal defects and the possible transitions with emission wavelengths are